Journal of Applied Mechanics and Technical Physics, Vol. 36, No. 3, 1995

MASS EXCHANGE IN GAS DESORPTION FROM FINELY DISPERSED LIQUID PARTICLES IN A NEAR-WALL TWO-PHASE JET

V. P. Lebedev, V. I. Terekhov, and N. E. Shishkin

UDC 532.529:536.24:536.423

Experimental results [1, 2] suggest that the delivery of finely dispersed particles into the near-wall flow region leads to a significant improvement in protection properties of a gas screen. This is accounted for by the additional heat extracted from the hot flow in order to heat and evaporate the liquid particles.

In the task under consideration (Fig. 1), a dispersed liquid jet and an air flow are delivered into the near-wall region of the channel through a tangential slot. In this case a two-phase air–liquid jet develops in the conjugate air flow, moving in the channel center at a velocity differing from that of the jet.

The picture of the interaction of the two-phase gas-liquid jet with the conjugate flow and the channel is very intricate. Many factors determine the heat and mass exchange processes between the particles and the gas flow. The main ones are as follows: the particle concentration and their dispersed composition, hydrodynamic structure of the flow, as well as processes of coagulation and particle deposition on the wall with formation of nonstationary wave-shape films on the surface. A theoretical description of the task is extremely difficult, and even for simpler cases, e.g., for gas–liquid flow in a tube [3–5], the authors use a series of simplifying assumptions that need experimental confirmation.

This work deals with the experimental investigation of the mass exchange between finely dispersed liquid particles and a gas flow. We investigate mass transfer in the desorption process of a slightly water-soluble carbonic acid gas from the liquid particle surface at wide variations of the rate parameters for both gas and liquid phase. These data may be further used in the analysis of heat and mass transfer processes in near-wall two-phase flows.

The possibility of absorption–desorption processes to be intensified in a two-phase gas-liquid particle flow is another important applied aspect of the given task. The interface for the gas-liquid particle flow may be much larger than the phase interface in the film flow regime frequently used in absorbers [6].

Mass transfer from the liquid film surface in gas absorption–desorption process has been experimentally investigated in detail [7, 8], but at the same time there is a lack of published work dealing with two-phase near-wall flow. This paper attempts to fill this gap.

1. The Experimental Technique. The experiments were conducted by using the same set-up, on which heat efficiency of two-phase near-wall jets was studied [1]. Figure 1 presents a scheme of the set-up. The horizontally situated working region consists of a cylindrical channel of 100 mm inner diameter and 1200 mm length.

On the channel inlet there is a tangential circular slot 5 mm in height, through which a gas–liquid near-wall jet was delivered. For comparison, a set of experiments was conducted at the liquid film delivery along the channel wall. In this case the circular slot height was $s = 0.5$ mm.

The liquid spraying into the near-wall jet was maintained by water injection through 48 capillaries with inner diameter 0.5 mm, uniformly situated along the circular slot. The capillaries were mounted at approximately half-height of the slot. Upon such injection, the water mass concentration $K_l = G_l/(G_a + G_l)$

Institute of Thermophysics, Russian Academy of Sciences, Novosibirsk 630090. Translated from Prikladnaya Mekhanika i Tekhnicheskaya Fizika, Vol. 36, No. 3, pp. 122–129, May–June, 1995. Original article submitted April 5, 1994.

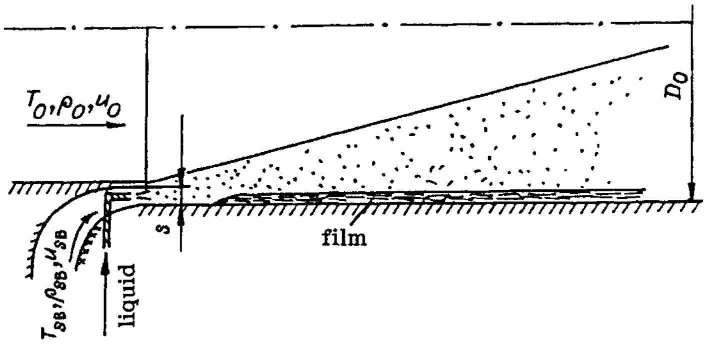

Fig. 1

may be changed in a wide range: $K_l = 0 \div 0.5$ (G_l and G_a are rates of the gas and liquid phases injected into the near-wall jet).

Experimental investigations were made in a wide range of regime parameters. The velocity of the main flow at the working region inlet was $u_0 = 25 \div 65$ m/sec and the Reynolds number was $\mathrm{Re}_0 = u_0 D_0/\nu = (1.5\text{–}4.3) \cdot 10^5$. An air flow with temperature $T_0 \approx 290$ K was used as the main flow; the air and the liquid injected into the near-wall jet had the same temperature ($T_s \approx T_0$). The injection parameter was determined by average-rate values of the mass velocity for the gas and liquid phases at the circular slot section: $m = \rho_s u_s/\rho_0 u_0$ ($\rho_s u_s = (G_a + G_l)/F_s$, F_s is a circular slot area). During the experiments the injection parameter varied in the range $m = 0.5\text{–}1$.

The dispersed composition and calculated concentration of the liquid particles injected into the channel were not studied in detail. However, visual observations, photoregistration, and an estimation of particle sizes by their deposition on special substrates show that the diameter of the injected particles does not exceed $d_s < 100\text{–}200$ μm, and there were no large particles in the flow.

Experimental investigations were accompanied by visual observation over the process of development and mixing of the near-wall two-phase flow. In this case the channel walls were made of transparent material. It was found that the liquid running along the tubes inside the circular slot was spraying rapidly, forming a uniform circular water dust layer practically at the initial section. A sufficiently high particle concentration in a thin layer of the dispersed liquid initiates its deposition on the wall, accompanied by liquid film formation. The birthplace of the film formation and the coordinates of its disruption and breakdown from the surface were registered during the experiments.

The axial symmetry of the film formed on the channel walls was important during the experiments. Gravitational forces may lead to liquid overflow into the lower part of the cylindric channel. However, visual observations and special measurements of adiabatic surface temperature at separate points along the channel circumference [1] confirm that overflow effects have no practical influence. The uniform film thickness along the circumference is due to the high value of the main flow velocity u_0 in the experiments. As the velocity decreases ($u_0 < 25$ m/sec), the axisymmetric character of the film flow breaks down.

During the experiments mass transfer was measured durind desorption of slightly water-soluble carbonic acid gas. Preliminary water saturation by carbonic acid gas was made by CO_2 barbotage through a liquid layer in a tank. Gas was dissolving in water during several hours, thus the CO_2 concentration in the whole water volume was nearly constant. Gas-saturated liquid runs from the tank into the working region of the setup by the method of exclusion. The saturated gas concentration on the channel inlet was $C_s \approx 500\text{–}800$ mg/liter.

The saturated gas concentration was determined by the method of special analysis [9]. Carbonic acid neutralization was accomplished using caustic soda. Probes were made along the whole length of the working region, and for this purpose the channel was made of separate sections, which formed the length of the channel. This helped to trace gas concentration changes and mass transfer coefficients along the channel length. The maximum error in the concentration measurements when this method was used does not exceed 10%, according to [7].

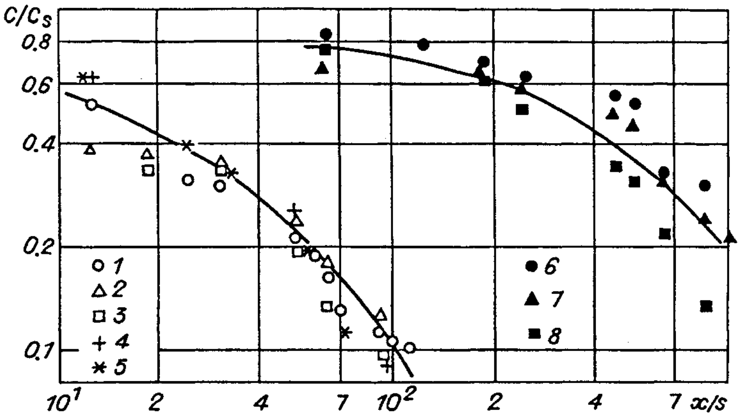

Fig. 2

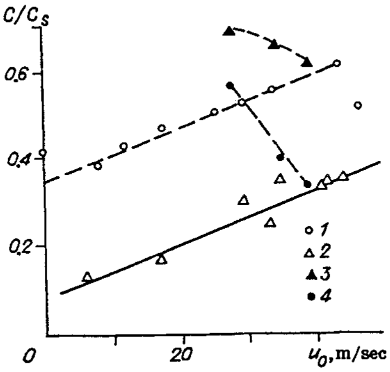

Fig. 3

2. Experimental Results and Discussion. A program of experimental investigations includes investigations on the influence of the mass concentration of the liquid phase on mass transfer with variations of the air rate in the near-wall jet and in the main flow. The dispersed composition of the spraying liquid during the experiments remained constant. The maximum value of liquid concentration reached $K_l = 1$, which corresponded to the liquid film supply into the channel. These experiments anabled a direct comparison of mass transfer intensification in liquid spraying with the film flow regime.

Figure 2 shows the changes in saturated carbonic acid gas concentration C along the channel length, where points *1*–*5* correspond to the spread liquid and points *6*–*8* to a liquid film. The regime parameters for the points in Fig. 2 were the following: $m = 0.68$, $K_l = 0.22$, $u_0 = 29.4$ for point *1*; 0.74, 0.26, 34.4 for point *2*; 0.73, 0.24, 42.0 for point *3*; 0.77, 0.24, 43.6 for point *4*; 0.74, 0.24, 44.1 for point *5*; $m = 8.1$, $G_l/G_0 = 0.17$, $u_0 = 27.5$ for point *6*; 6.45, 0.13, 34.4 for point *7*; 5.8, 0.12, 38.1 for point *8*. The injection parameter ($m \approx 0.7$) and mass concentration of liquid particles at the inlet ($K_l \approx 0.25$) for the gas–liquid jet were kept constant during the present series of experiments. During the experiments with the liquid film (points *6*–*8*) the injection parameter and the ratio of film to main flow rates were also nearly constant. Moreover, the flow rates of the liquid injected into the channel are close in value for the gas–liquid jet and for the film.

As seen in Fig. 2, the desorption process in the gas–liquid near-wall jet was running more intensely than during gas desorption off the liquid film surface. This process was the most active in the initial site of the channel ($x/s < 10$–20), where, according to visual observations, a region with finely dispersed particles exists. The CO_2 concentration along the channel in the liquid film decreases more slowly than in the gas–liquid jet, thus confirming that mass-transfer processes in the film flow regime become weaker.

Instability of the air velocity in the main flow is one of the causes of the spread of experimental data in Fig. 2. Figure 3 illustrates the influence of this parameter on the gas desorption process. Here points *1* and *2* correspond to the gas-liquid jet ($K_l = 0.3$; $x/D_0 = 0.63$ for point *1*; $K_l = 0.24$; $x/D_0 = 1.53$ for point *2*) and points *3* and *4* to the liquid film ($K_l = 1$; $x/D_0 = 0.93$ for point *3*; *4* — $K_l = 1$; $x/D_0 = 2.3$ for point *4*).

In the given run of experiments the flow rate of gas and liquid phase through the circular slot was constant, and only the velocity of the main flow changed. The character of the influence of main flow velocity on the desorption process in a gas–liquid medium differs greatly from the film flow. The increase in velocity u_0 under otherwise identical conditions leads to C/C_s growth or to decreased mass transfer processes. On the contrary, at the liquid film flow the increased air velocity of the main flow leads to intensification of mass transfer off the film surface. This opposite influence of velocity u_0 on the gas concentration is determined by a complex mixing mechanism of a two-phase near-wall flow with the main flow. Actually, for the film flow regime the increase in conjugate flow velocity u_0 leads to growth in the relative velocity of the overflow and to increased desorbing gas flow off the film surface.

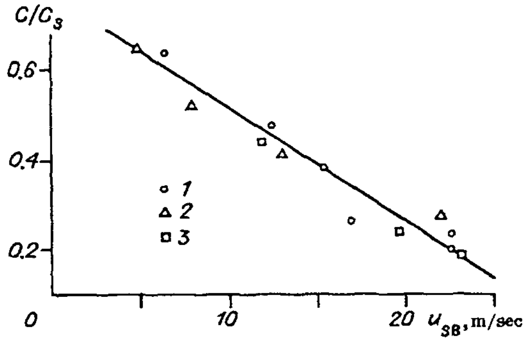

Fig. 4

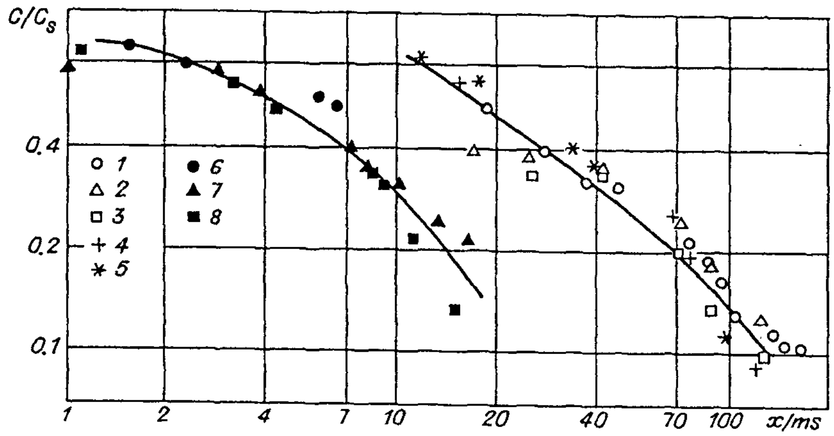

Fig. 5

At the gas-liquid jet flow the increased velocity of the main flow leads to a decrease in injection parameter m, which in turn, initiates a decrease in velocity gradients and weakening of mixing processes in the jet boundary layer. Moreover, an increase in the parameter m (in experiments starting from $m = 5$ at $u_0 \approx 10$ m/sec to $m = 0.8$ at $u_0 = 42$ m/sec) leads to thinning of the near-wall jet and an increase in coagulation processes, which cause a decrease in mass transfer.

Unlike the increased velocity in the gas-liquid near-wall jet, the velocity in the main flow leads to considerable intensification of the mass-transfer processes. This is clear in Fig. 4 which shows experimental data obtained under received at the following regime conditions: points *1–3* correspond to $u_0 = 29$, 35, and 42 m/sec; the liquid concentration at the inlet and the distance from the channel edge were fixed ($K_1 \approx 0.3$, $x/D_0 \approx 1$). As seen, the influence of the velocity u_s influence in the whole investigated range and the type of dependence $C/C_s = f\ (u_s)$ are approximately linear.

When the influence of velocity ratios in the jet and in the main flow is taken into account, the experimental data on concentration distribution along the channel can be to better generalized. Figure 5 presents experimental results in the form of the ratio $C/C_s = f(x/ms)$. This treatment provides smaller scattering of experimental points for both the gas-liquid and film flow regimes, compared with analogous data presented in Fig. 2, which do not take into account velocity changes in the main flow and in the near-wall jet. The designation of points in Fig. 5 correspond to that in Fig. 2.

The concentration of the liquid phase is one of the important parameters that determine the desorption processes in a two-phase jet. Figure 6 shows the influence of the liquid concentration on CO_2 desorption for a fixed section $x/D_0 \approx 1$ (points *1–3* correspond to air velocity in the main flow $u_0 = 29$, 34, 42 m/sec). An increase in liquid amount in the near-wall jet leads to weakening of the mass transfer process between

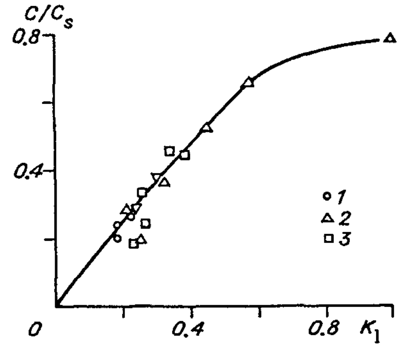

Fig. 6

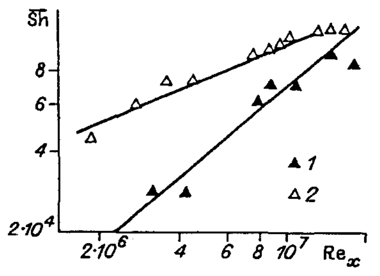

Fig. 7

the liquid and the air flow. The influence of the liquid phase concentration on the desorption process is very significant. Thus, the increase in liquid content in the jet from $K_l = 0.2$ to 0.6 leads to a greater than threefold growth in carbonic acid gas concentration in the liquid or to the same decrease in the average mass transfer coefficient.

In the the next step the experimental data were treated in the criterion form. Large difficulties appear in determining the mass transfer coefficient for the gas–liquid mixture flow. In the given case the gas–liquid near-wall jet appears in the form of an equivalent liquid film with a rate equal to the liquid phase rate, and with a mass transfer interface equal to the surface of this film. This presentation of experimental data is justified by the fact that it helps to make a direct comparison of the mass transfer in the near-wall gas–liquid flow with the mass transfer in the film flow regime. With the above information taken into account, the mass transfer coefficient in the experiments has the following form:

$$\beta = j_w/(C - C^*), \tag{2.1}$$

where j_w is the length-averaged cross flow of the desorbing gas; C is the CO_2 concentration in the liquid in the current section; C^* is the equilibrium concentration on the film surface. For the experiments conducted, this value was negligibly small ($C^* \approx 0$). Then the length-averaged mass transfer coefficient was determined on the basis of ratio (2.1) using the formula

$$\overline{\beta} = (C_s - C)q/\overline{C}x.$$

Here $q = u_s s = G_l/\pi D_0 \rho_l$ is the liquid volume rate per unit of film width; $\overline{C} = (C_s + C)/2$ is the average concentration on length x.

The Sherwood number in the experiments was calculated by using the average value of the mass transfer coefficient $\overline{\mathrm{Sh}} = \overline{\beta}x/D$, the molecular coefficient of carbonic axid gas diffusion in water $D \approx 1.9 \cdot 10^{-9}$ m^2/sec, and the Schmidt number $\mathrm{Sc} \approx 530$.

The Reynolds number was determined from the velocity difference between the equivalent film and the air flow: $\Delta u = u_0 - u_{\text{film}}$. Thus we take into account the phase drift, which reflects the peculiarities of film mass transfer in high-velocity air flow. The longitudinal coordinate x was used as a linear scale. Then $\mathrm{Re}_x = \Delta u x/\nu_l$.

Figure 7 presents the experimental results in the form Sh versus Re_x. Point *1* ($G_l = 0.042$ kg/sec, $K_l = 1$, $u_0 = 28$ m/sec) corresponds to liquid film injection into the channel, and point *2* corresponds to gas–liquid jet injection ($K_l = 0.22$, $u_0 \approx 28$ m/sec).

Analyzing Fig. 7, we draw the following main conclusion: there is a significant (more than twice) increase in the mass transfer coefficient in the initial section of the channel for the gas–liquid jet in comparison to the film flow regime. Further down the flow, when the dispersed water dust starts to settle on the channel wall, the mass transfer intensification for both investigated flow regimes became closer to each other. Visual observation of the film formation character at dispersed liquid delivery into the channel is another confirmation of this.

The increase in the interface during the flow of a liquid drop–air mixture is the main cause of mass transfer intensification in the initial site. Simple estimations show that for monodispersed 100 μm drop composition the ratio of the interface for gas-drop flow and liquid film is $F_s/F_{\text{film}} \approx 3 \cdot 10^3$. However, one should take into account that the mass transfer coefficient directly on the drop surface is much lower than the mass transfer on the film surface because of the small relative velocities of the phase slip. The influence of these two factors leads to a more than twofold growth of mass transfer in the near-wall gas–liquid jet as compared with the film flow.

Thus, the experimental investigations conducted show a significant intensification of mass transfer in the near-wall gas–liquid jet, as compared with the film liquid flow regime. The air velocity of the main flow and the velocity and concentration of the liquid phase in the near-wall jet have a strong influence on the intensity of the mass transfer processes. The data obtained may be the basis for testing theoretical models of mass transfer in a two-phase gas-drop flow. However, the lack of experimentally found dispersed composition of liquid drops and their numerical concentration at the inlet may complicate the problem of comparison of numerical and experimental results. Thus, experimental determination of the mentioned parameters and also gas and particle velocities turn out to be important for further investigation of heat and mass transfer in conjugate two-phase near-wall jets.

In conclusion the authors express their gratitute to O. A. Borisova for help in the experimental investigations.

This work was supported by the Russian Foundation for Fundamental Research (Grant 94-02-03222-a).

REFERENCES

1. E. P. Volchkov, V. P. Lebedev, V. I Terekhov, and N. E. Shishkin, "Experimental investigations of the influence of finely dispersed liquid drop concentration on the efficiency of a gas screen," Sib. Fiz.-Tekh. Zh., **1** (1992).
2. V. M. Repukhov and A. I. Neduzhko, "Heat protection of a wall by two-phase gas-liquid cooler injection," Dokl. Akad. Nauk Ukr. SSR, Ser. A, No. 8 (1988).
3. Sh. Yo, "Convective heat transfer in the region of laminar flow stabilization in tubes with round section," Trans. ASME, J. Heat Transfer, **101**, No. 3 (1979).
4. Sh. Yo and A. Rein, "Heat transfer during laminar flow of a finely dispersed vapor–liquid mixture," Trans. ASME, J. Heat Transfer, **102**, No. 4 (1980).
5. Ganic, Rosenou, "A mechanism of drop deposition in a dispersed two-phase flow," Trans. ASME, J. Heat Transfer, **101**, No. 2 (1979).
6. V. M. Ramm, Gas absorption [in Russian], Chemistry, Moscow (1966).
7. S. V. Alekseenko, V. E. Nakoryakov, and B. G. Pokusaev, Wave Flows of Liquid Films [in Russian], Nauka, Novosibirsk (1992).
8. N. M. Kulov, V. V. Maksimov, V. A. Malusov, and N. M. Zhavoronkov, "Mass transfer in draining liquid films," Teor. Osn. Khim. Tekhnol., **17**, No. 3 (1983).
9. E. V. Alekseevsky, R. K. Golts, and A. P. Musakin, Numerical Analysis [in Russian], Goskhimizdat, Leningrad (1955).